Mon. Not. R. astr. Soc. (1980) **193**, 793–824

Theory and observations of the optical continuum and line spectra of accretion discs around white dwarfs

S. K. Mayo *Royal Greenwich Observatory, Herstmonceux Castle, Hailsham, Sussex BN27 1RP and Institute of Astronomy, Madingley Road, Cambridge CB3 0HA*

D. T. Wickramasinghe *Royal Observatory, Blackford Hill, Edinburgh EH9 3HJ*

J. A. J. Whelan *Institute of Astronomy, Madingley Road, Cambridge CB3 0HA*

Received 1980 April 25; in original form 1979 November 5

Summary. Theoretical calculations of the optical continuum ($\lambda \gtrsim 3000$ Å), *UBV* colours and Hα, Hβ and Hγ absorption line profiles are presented for steady-state accretion discs around white dwarfs. Several approximations (in particular with regard to the atmospheres) are made and discussed. The uncertainties with regard to disc Z-structure and outer boundary are considered. The effects of varying the inclination angle, mass of the white dwarf and mass flux rate through the disc are discussed. The theoretical results are compared with observations of *UBV* colours obtained from the literature and with line profiles reported here of dwarf-novae in outburst and UX UMa 'disc' stars. In general the overall agreement between theory and observations is good for the *UBV* colours and reasonable for the line profiles. Comparison between the outburst and the superoutburst properties of dwarf novae suggests that the mass flux rate is of order four times larger during the superoutbursts.

Comparison is also made with the theoretical disc spectra results of Schwarzenberg-Czerny & Rózyczka and Herter *et al.* Reasonable agreement is found and reasons are suggested for the overall differences between some of those models and the ones reported here.

1 Introduction

There is evidence that many close binary systems contain accretion discs (e.g. Gorbatskii 1964; Smak 1971; Warner 1976a; Robinson 1976). For the X-ray binary systems and cataclysmic variables the disc can be observed directly as it dominates the output of radiation in certain wavebands (Pringle & Rees 1972; Warner 1976a, b; Bath *et al.* 1974).

In this paper we consider accretion discs around white dwarfs. We calculate the emergent optical continuum, *UBV* colours and hydrogen-line absorption spectrum and compare the results with observations. In general such a computation is very complicated and we have made several simplifying assumptions. Nevertheless the results may be applicable to a sub-

set of observed discs, in particular to the UX UMa disc stars (Warner 1976b), and certain dwarf novae at or near outburst, and possibly at quiescence. The comparison of observations and theory will be a further test of the disc model for dwarf novae (Smak 1971; Bath *et al.* 1974).

The problem essentially consists of three parts: (i) a model for the physical structure of the disc which gives values everywhere for effective temperature (T_e) and vertical gravity (g_z); (ii) given T_e and g_z a model for the emergent intensity as a function of inclination angle, i; and (iii) the sum over the disc of the computed intensities (properly weighted by area and with Doppler velocity shifts included), from which continuum colours and line profiles can be calculated.

Since the exact physical structure of the disc is uncertain we have adopted the simplest case which has the fewest free parameters – the steady state disc. Because of this fundamental uncertainty we have used very simple models to treat the stellar atmospheres. We computed our own atmosphere models, rather than interpolate in published grids of stellar atmospheres, because: (i) in general the range of (T_e, g) parameters of a disc is not well covered by published grids at given chemical composition; (ii) we are interested in the emergent intensity in a specific direction, $I_\nu(\mu)$, rather than the integrated emergent flux, F_ν; and (iii) we wish to calculate detailed absorption line profiles.

Three aspects of the present problem, which we have considered but not solved in detail are the optical thickness of the disc, its Z-structure and where its outer boundary, R_2, should be. We discuss our approach in theoretical outline in Section 3 and in the light of observational constraints in Sections 7 and 8. We note that for a stellar atmosphere calculation to be meaningful the disc must be optically thick. This assumption is supported by observation of broad shallow absorption lines in dwarf novae spectra during outburst (Elvey & Babcock 1943) and in UX UMa stars. Warner (1976a), Robinson (1976) and Whelan, Rayne & Brunt (1979) have summarized the evidence for believing that such lines originate in the disc rather than elsewhere in the system. Indeed one motivation for the present calculation of disc hydrogen absorption lines was to see if the theoretical line profiles agree with the observed ones.

In this paper we do not consider the marginally optically thick or optically thin parts of the disc. These parts are probably of electron densities, n_e, in the range $10^9 \lesssim n_e\,(\mathrm{cm}^{-3}) \lesssim 10^{14}$ and are responsible for part or all of the emission line spectrum. At such densities the low density nebular type recombination calculations (e.g. Osterbrock 1974) are not valid and the emission line spectrum cannot be simply superposed on the model disc absorption spectrum; instead a detailed atomic physics and radiative transfer calculation has to be done (e.g. Williams 1980).

In Section 2 we discuss other work on the spectrum of an accretion disc in order to put the present work in context. Sections 3 and 4 contain the details of the disc model and atmosphere model, and Section 5 describes the procedure used for calculating *UBV* colours. Sections 6 and 7 contain the continuum and colour results and a comparison with observations. Section 8 describes the line profile calculation and the comparison with our observations. Section 9 contains our conclusions. A brief outline of part of this work was presented at *IAU Colloquium 46, New Trends in Variable Star Research,* Hamilton, New Zealand, 1978 (Mayo *et al.* 1979). In that paper in Table 1 the values of F should be 60 and 0.6 instead of 50 and 0.5 and in Table 2 Hα and Hγ should be interchanged.

2 Recent and current studies of accretion disc spectra

Table 1 summarizes the details of recent work. Lynden-Bell (1969) showed that a steady-state blackbody disc has a power law (thermal) spectrum $F_\nu \propto \nu^{1/3}$, in the case that $R_2 \gg R_1$

and for $kT_2 \ll h\nu \ll kT_1$ where R_1 is the inner boundary and R_2 the outer boundary of the disc, and T_1 and T_2 are the corresponding temperatures. If R_2 is not $\gg R_1$ then there is a spectrum $F_\nu \propto \nu^{1/3}$ approximately over a limited frequency range, with turnovers at each end (e.g. Shakura & Sunyaev 1973; Pringle 1974). F_{16} is the mass flux rate through the disc in units of $10^{16}\,\mathrm{g\,s^{-1}}$.

There is general agreement in the results derived from blackbody treatments. Pacharintanakul & Katz (1980) discuss also the effects of reprocessing X- and UV-radiation and show it to be negligible in the case when the central object is a white dwarf. Tylenda (1977) showed that for typical disc parameters at $\lambda > 2000\,\text{Å}$, the bright spot and the boundary layer are unimportant compared with the disc during outburst. However, during quiescence the disc may not be dominant.

The studies involving stellar atmosphere calculations involve more parameters which lead to a larger variety of results. As far as can be determined there is broad overall agreement among the results, but there are several differences of detail which show up especially in the comparison with observations. Most of the differences in results can be attributed to the different values assumed for $Z_0(R)/R$ and R_2. We discuss in Sections 7 and 8 the sensitivity of the results to changes in these parameters and we note that observational constraints may be more useful than theoretical ones.

3 The disc model

The detailed physical structure of an accretion disc in general depends on several parameters, including the viscosity which is uncertain to several orders of magnitude.

3.1 STEADY-STATE DISC

For simplicity we consider a steady-state, thin accretion disc for which the mass flux rate, F, through the disc is constant. The steady-state assumption restricts the range of validity of the calculations and hence also the comparison with observations. The thin assumption means that the radial temperature gradient is much less than the vertical one, so that radiation leaks out vertically much faster than it is transported radially. This implies that each annulus can be treated separately.

Consider cylindrical polar coordinates (R, ϕ, Z) centred at the centre of the compact (white dwarf) star. The effective temperature $T_e(R)$ and vertical component $g_Z(R)$ of a steady state disc are given as

$$T_e(R) = \left[\frac{3GM_* F}{8\pi\sigma R^3}\left(1-\left(\frac{R_1}{R}\right)^{1/2}\right)\right]^{1/4}, \tag{1}$$

$$g_Z(R) = \frac{GM_* Z_0(R)}{R^3}, \tag{2}$$

(cf. Pringle 1974; Shakura & Sunyaev 1973; Novikov & Thorne 1973; Pringle & Rees 1972) where the self gravity of the disc has been neglected and M_* is the mass of the central object, R_1 is the inner radius of the disc, and $Z_0(R)$ is the disc thickness at radius R. For typical disc parameters ($M = 1\,M_\odot$, $F = 10^{16}\,\mathrm{g\,s^{-1}}$, $Z_0(R)/R = 0.05$, $R_1 = 10^9\,\mathrm{cm}$), the values of (T_e, g_Z) lie between main sequence and white dwarf values.

Table 1. Summary of calculations of the spectra of a steady-state accretion disc.

Author	Calculation of emergent radiation	Limb darkening procedure	$Z_0(R)/R$	Outer radius of disc
Lynden-Bell (1969); see also Pringle & Rees (1972), Shakura & Sunyaev (1973)	Blackbody	—	—	—
Bath *et al.* (1974)	Blackbody	—	—	$R_2 = 1.4\times10^{10}$ cm $T_2 = 5241\,F_{16}^{1/4}$ K
Tylenda (1977)	Blackbody	—	—	Various values of R_2 an $R_2 \leqslant R(T = 10^4\,\mathrm{K})$
Steiner (1979)	Blackbody	—	—	$R_2 = 2\times10^{10}$ cm
Schwarzenberg-Czerny & Rózyczka (1977)	Interpolation in grids of published stellar atmospheres Blackbody at $T > 6\times10^4$ K	From published tables	0.01	Various values of R_2 bu $T_2 \lesssim 4000$ K often
Kiplinger (1977, 1979)	Interpolation in grids of published stellar atmospheres	Eddington approximation	~0.05	Various values of R_2 adjusted to fit observati
Robinson *et al.* (1978)	—	—	—	—
Pacharintanakul & Katz (1980)	Blackbody	—	0.01	$R_2 = 10^{10.5}$, 10^{11}, $10^{11.5}$ cm
Herter *et al.* (1979)	Model atmospheres	$I_\nu(\mu)$ calculated at various μ	0.01	$8.6\times10^9 \leqslant R_2\,(\mathrm{cm}) \leqslant 2\times10^{10}$
Present paper (see also Mayo *et al.* 1979)	Approximate atmospheres computed directly Grey T–τ approximation Full frequency-dependent opacities	$I_\nu(\mu)$ calculated at various μ	0.05 0.01	Various test values of R_2 and $R_2 = R(T = 10^4\,\mathrm{K})$

3.2 $Z_0(R)$

The thickness of the disc, $Z_0(R)$, is determined by the balance between the vertical pressure gradient and the Z component of gravity from the central object. (The R-component of gravity is balanced by centrifugal force owing to the rotation of the disc, *cf.* Fig. 1.) Lynden-Bell & Pringle (1974) have discussed very approximate analytic expressions for $Z_0(R)$ and

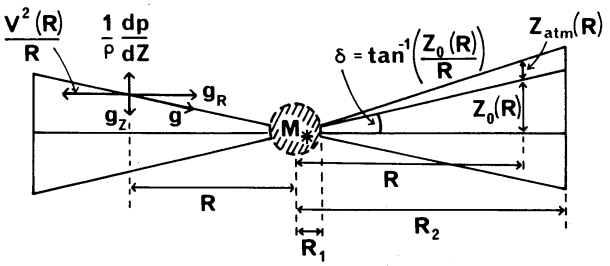

Figure 1. Schematic cross-section of a disc illustrating quantities referred to in the text. The left hand side shows the forces per unit mass acting at a point on the disc's surface. The right hand side shows certain disc parameters. (δ and Z_{atm} (R) are exaggerated for clarity.)

culations presented of ours	Continuum	Lines	Comments
	($F_\nu \propto \nu^{1/3}$)	—	—
ical > 3500 Å)	—	—	Bright spot considered
	√	—	Bright spot and boundary layer considered; UV and X-ray emission calculated.
V	√	—	Boundary layer included
V	—	—	—
	√	Interpolation in published grids	—
	—	Broadening with typical disc velocities of Wickramasinghe's (1972) white dwarf profiles	—
V	√	—	Reprocessing and R_1 small (neutron star) considered
V, uvby	√	Vidal *et al.* (1973) broadening theory and rotational Doppler broadening for hydrogen lines	—
V	√	Griem (1964) theory and rotational Doppler broadening for hydrogen lines	—

Pringle (1974) has argued that, over a limited range of R, $Z_0(R)/R \sim$ constant. We have adopted the expression

$$Z_0(R)/R = \text{constant}. \tag{3}$$

where for most models the constant was 0.05.

We note that choosing $Z_0(R)/R =$ constant is equivalent to choosing the viscosity parameter α (in this case as a function of R) in the α-models of Shakura & Sunyaev (1973). Their equation (2.19) gives

$$Z_0(R)/R \sim 0.01\,\alpha^{-0.1}\,F_{16}^{0.15} \tag{3a}$$

where $M = 1\,M_\odot$ and $R = 10^{10}$ cm. For $F_{16} = 1$, $\alpha \sim 1$ and 10^{-7} give $Z_0(R)/R \sim 0.01$ and 0.05 respectively. For $F_{16} = 100$, $\alpha \sim 1$ and 10^{-4} give $Z_0(R)/R \sim 0.02$ and 0.05 respectively.

The value of $Z_0(R)/R$ can affect the optical thickness of the disc (Section 3.4). Its only effect on the formal computations is in $g_Z(R)$ by equation (2). The value of g_Z affects the emergent continuum radiation only slightly but does significantly affect the amount of Stark (pressure) broadening in the line profiles.

3.3 INNER DISC BOUNDARY

If the central object is rotating much slower than break-up (Keplerian) velocity, and if it has negligible magnetic field, then the radial size of the boundary layer where the disc grazes the star is small (Pringle 1977). The inner radius of the disc is then approximately the stellar radius which is essentially a function of the stellar mass (neglecting composition effects). We adopt

$$R_1 = R_* = R_*(M_*). \tag{4}$$

Any error here has a small effect on the emergent optical radiation field since although the material is hot it occupies a small area.

3.4 OPTICAL DEPTH THROUGH THE DISC

Since the aim of the present work is to calculate the emergent radiation field from the optically thick part of the disc we investigate if the disc is optically thick. The optical depth in a vertical direction through the disc is given by

$$\tau_Z(R) = 2\int_{Z=0}^{Z=Z_0(R)} \kappa\rho\, dZ, \tag{5}$$

where $\rho(Z)$ is a function of the viscosity. This integral has been evaluated by Shakura & Sunyaev (1973) for the α-model discs. Using their equations (2.16) and (2.19) for τ we find that for the worst case

$$\tau_Z \sim 3.6\,\alpha^{-4/5} F_{16}^{9/10}. \tag{6}$$

This suggests that for $\alpha \ll 1 (Z_0(R)/R \sim 0.05)$ the disc will be optically thick everywhere. Expression (6) does, however, raise the possibility that for $\alpha \sim 1 (Z_0(R)/R \sim 0.01)$ there may be some regions of the disc where its optical thickness is in doubt.

We have further investigated the problem of the self-consistency of the disc with regard to optical depth by calculating γ, where

$$\gamma = \frac{Z_{\rm atm}\,[T_{\rm e}(R), g_Z(R)]}{Z_0(R)}, \tag{7}$$

where $Z_{\rm atm}$ is the physical depth of a stellar atmosphere, with parameters $T_{\rm e}$ and g_Z, down to $\tau = 1$ (see Fig. 1).

If $\gamma \ll 1$ then the disc is optically thick and the change in the vertical component of gravity over the length $Z_{\rm atm}$ is small compared with the disc height Z_0. Then we can consider each disc annulus as having a stellar atmosphere on top with $T_{\rm e}(R)$ and $g_Z(R)$ given by equations (1) and (2), and, moreover, $g_Z(R)$ can be taken as a constant in the stellar atmosphere calculation. If $\gamma \gg 1$ then the depth of the atmosphere is larger than Z_0 so the disc is essentially optically thin. If $\gamma \sim 1$ the disc is probably just optically thick but the large extent of the atmosphere causes $g_Z(R)$ to be no longer constant with height in the stellar atmosphere.

Table 2 gives some values for γ and other disc parameters such as $T_{\rm e}$ and $\log g_Z$ for typical discs. It can be seen that $\gamma \sim$ constant through any given disc. This is in agreement with the weak dependences of τ etc. on disc parameters found by Shakura & Sunyaev (1973) and can also be confirmed analytically (Mayo 1980). Table 2 shows that, for $Z_0(R)/R = 0.05$, $\gamma \ll 1$ and the disc is optically thick. However, for $Z_0(R)/R = 0.01$, $\gamma > 1$ at the high

Table 2. Values of $\gamma = Z_{\rm atm}(R)/Z_0(R)$ for places in discs. $M_* = 1.0 M_\odot$ $R_1 = R_* = 10^9$ cm.

$\frac{Z_0(R)}{R}$	R (10^9 cm)	$T(R)^\star$ (K)	$\log g_Z(R)$ cgs	$Z_{\rm atm}(T_e(R), g_Z(R))$ 10^8 cm	$Z_0(R)$ 10^8 cm	γ
				$F = 6\times10^{15}$ g s^{-1}		
0.05	1.77	16089	6.325	0.016	0.885	0.018
	4.27	10222	5.56	0.050	2.135	0.024
	9.87	5965	4.83	0.174	4.935	0.035
0.01	1.77	16089	5.62	0.126	0.177	0.71
	4.27	10222	4.86	0.294	0.427	0.69
	9.87	5965	4.13	0.85	0.987	0.87
				$F = 6\times10^{17}$ g s^{-1}		
0.05	2.97	39922	5.88	0.214	1.48	0.14
	8.67	20564	4.94	0.760	4.34	0.18
	24.57	10092	4.04	2.45	12.3	0.20
	49.00	6199	3.44	4.16	24.5	0.17
0.03	2.97	39922	5.65	0.388	0.89	0.44
	8.67	20564	4.72	1.35	2.60	0.52
	24.57	10092	3.82	4.36	7.35	0.59
	49.00	6199	3.22	6.90	14.6	0.47
0.01	2.97	39922	5.18	1.32	0.297	4.4
	8.67	20564	4.24	4.78	0.867	5.5
	24.57	10092	3.34	15.3	2.46	5.6
	49.00	6199	2.74	20.8	4.90	6.2

*The values of $T(R)$ are actual values used for atmospheres. They are a little different from those derived from equation (1) owing to the use of discrete temperature annuli in the disc (Section 4.1).

mass flux rate shown. This indicates that there may be problems of optical thinness in such a disc or that the consistency of the $Z(R)/R = 0.01$ constant approximation with the actual disc has broken down (i.e. α has become larger than unity).

3.5 THE DISC OUTER BOUNDARY

It is difficult to find a criterion for choosing R_2, the outer disc boundary. Table 2 and Shakura & Sunyaev (1973) show that estimates of optical depth are largely independent of R and hence 'going optically thin' does not provide a sharp criterion for the disc edge in the present model, though this may be what actually occurs. In a real disc, of course, the $Z(R)/R$ = constant approximation breaks down in the outer regions where the matter density becomes low. Further, in a binary system the disc size is limited by the Roche lobe and by tidal effects. Observations indicate disc sizes of order $1-10\times10^{10}$ cm. We note that a very rough approximation is to cut the disc off at $T_e = 10^4$ K (Pringle 1974; Tylenda 1977).

In view of the lack of a practical criterion to detemine R_2, we have constructed model discs with R_2 as a free parameter.

3.6 SUMMARY

A simple disc model is used. The parameters to be specified are M_*, F, R_2 and the fixed value of $Z_0(R)/R$. R_1 is determined by M_*. The values chosen must be such that $\gamma \ll 1$.

In view of the tremendous uncertainties we calculate mainly quantities which are ratios (colours, lines) and we vary one disc parameter at a time to determine relative effects.

4 The atmosphere model

4.1 ANNULI

The disc is divided into a finite number of circular annuli with fixed T_e and g_Z. In reality T_e and g_Z vary across the width of an annulus and the widths were chosen to restrict the variations to be less than 5 per cent in T_e and 0.1 in $\log g_Z$. This requires typically 40 annuli per disc each of which is treated independently as regards constructing an atmosphere.

4.2 RADIATIVE TRANSFER AND ATMOSPHERE STRUCTURE

To determine the emergent intensity in each annulus we must solve the radiative transfer equation,

$$\mu \frac{dI_\nu}{d\tau_\nu} = I_\nu - S_\nu, \tag{8}$$

at a number of wavelength points in the range 2000–33 000 Å. Here ν is the frequency subscript, I_ν is the intensity (in erg s^{-1} cm^{-2} Hz^{-1} sr^{-1}), S_ν is the source function, τ_ν is the optical depth and $\mu = \cos\theta$ where θ is the angle between the normal to the disc and the line-of-sight.

To make the problem tractable we have made several approximations and assumptions. Note that the plane-parallel assumption normally used for spherical stellar atmospheres is actually correct in this flat disc case. We assume LTE and use the approximate Eddington distribution to describe the temperature–optical depth structure of the atmosphere

$$T^4(\tau_{\rm std}) = 0.75\, T_e^4(\tau_{\rm std} + 2/3), \tag{9}$$

where $\tau_{\rm std}$ is taken at a standard wavelength ($\lambda_{\rm std} = 4000$ Å for $T_e > 10\,000$ K and $\lambda_{\rm std} = 5000$ Å for $T_e \leqslant 10\,000$ K). The physical structure of the atmosphere is then calculated from the hydrostatic equilibrium equation

$$\frac{dP}{dZ} = -\rho g_Z, \tag{10}$$

where P is the pressure and ρ is the density. In equation (10) g_Z is constant and given by equation (2).

An essentially solar chemical composition was used. The proportions by number are $n(\mathrm{H}) = 0.908$, $n(\mathrm{He}) = 0.0908$, $n(\mathrm{rest}) = 1.18 \times 10^{-3}$. In 'rest' the 16 most abundant elements were included using abundances taken from Allen (1973) and Gingerich (1969).

Continuous opacity sources from, H, H^-, H_2^+, H_2^-, He, He^-, He^+ and scattering by free electrons and H, H_2 and He were incorporated. The frequency dependent temperature–optical depth scale is determined using full frequency dependent continuous opacities (Wickramasinghe 1971) from

$$\frac{d\tau_\nu}{d\tau_{\rm std}} = \frac{\kappa_\nu}{\kappa_{\rm std}}. \tag{11}$$

The source function S_ν is assumed to be the Planck function, B_ν, and scattering is neglected. For the continuum, scattering becomes important at high temperatures but for the lines scattering can contribute emission cores even at lower temperatures.

The solution of equation (8) is

$$I_\nu(\mu, \tau_\nu = 0) = \int_0^\infty \exp(-\tau_\nu/\mu) B_\nu(\tau_\nu) \frac{d\tau_\nu}{\mu}, \tag{12}$$

which is evaluated numerically using the quadrature of Cayrel & Traving (1960).

We have neglected the effects of convection. Calculations of the Z-structure of a disc (Pringle 1974) show that discs, in which electron scattering and radiation pressure are not dominant, are stable to convection. Such is the case for most parts of the discs we have considered. Convection becomes important at higher temperatures and lower gravities mainly due to radiation pressure effects. We note that calculations of model atmospheres by Gingerich (1969) show that in general convection has a small influence on the emergent flux distribution.

The full details of the numerical calculations and the tests of their accuracy are given elsewhere (Mayo 1980). Here we only summarize this aspect of the procedure. Flux constancy at each layer is not demanded in our atmosphere models and there are no iterations made to improve the T–τ function. This saved computer time. We find that for the ranges of T_e and g_Z of interest our simplifying assumptions lead to errors of order $\lesssim 20$ per cent in the emergent flux at optical and IR wavelengths ($\lambda > 3000$ Å) when compared with the flux constant atmosphere calculations of Gingerich (1969) and of Wickramasinghe (1972). The errors are much worse in the ultraviolet ($\lambda < 2000$ Å). The errors introduced by our simple atmosphere models into quantities involving *ratios* of intensities (e.g. colour indices, line profiles) are much smaller and of order $\lesssim 5$ per cent for $\lambda > 3000$ Å. Physically this is because the method used here gives essentially the correct frequency dependence but does not give the absolute intensities as it is not normalized by flux constancy. The assumption of LTE and $S_\nu = B_\nu$ is reasonably accurate in the disc case since when the temperature is high so is the gravity.

We did not try to improve to $\ll 5$ per cent accuracy in this part of the project because the (T_e, g_Z) grid is itself only accurate to of order 5 per cent and of course the disc model is only a steady-state approximation anyway.

Molecular and low temperature opacities were not included and thus our procedure fails below $T \sim 5000$ K.

4.3 THE INCLINATION i

The disc is seen by an observer at an angle i between the normal to the orbital plane and the line-of-sight. For simplicity we take i = constant for any given disc and neglect the $\pm\delta$

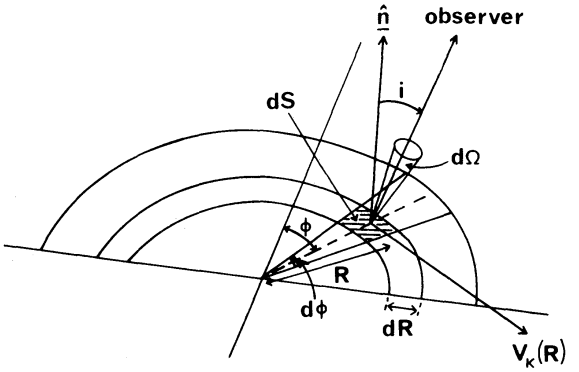

Figure 2. Geometry of disc annuli and sectors. The symbols are standard or defined in the text.

correction incurred because the disc is at an angle $\delta = \tan^{-1}(Z_0(R)/R)$ to the orbital plane (Fig. 1). For $Z_0(R)/R = 0.05$ and 0.01, $\delta = 3°$ and 0°.6. The correction is negligible except for $i > 80°$. Then $\cos i = \mu$ (*cf.* Fig. 2). We have calculated the emergent intensity for various values of i.

At large values of i (nearly edge-on discs) we observe radiation from higher up in the atmosphere (i.e. limb darkening). In this case the no scattering, LTE and $S_\nu = B_\nu$ assumptions become more severe. However, as far as discussing changes in disc parameters (colours etc.) as a function of i is concerned, these extra errors are not significant.

4.4 FLUX

The flux from the disc seen at Earth, $F_\nu(\mu)$ in erg s^{-1} cm^{-2} (of detector) Hz^{-1} is given by integrating the emergent intensity over the annuli of the disc

$$F_\nu(\mu) = \frac{2\pi\mu}{D^2}\int_{R_1}^{R_2} I_\nu(\mu, \tau_\nu = 0, R)\,R\,dR, \tag{13}$$

where D is the distance, which we have taken as 10 pc to standardize it. Note that there is no integrating over μ as there is for spherical stars.

4.5 BALMER LINES

For Hα, Hβ and Hγ the line opacity per atom in the appropriate state, $K_\nu(\Delta\lambda)$, as a function of $\Delta\lambda$, the wavelength with respect to the line centre, was computed using the Griem (1964) procedure. The oscillator strengths were obtained from Allen (1973) and the broadening function $R(N_e, T)$ was interpolated from the tables of Aller (1963).

4.6 TESTS

We summarize the main tests and checks made of our procedure. The full details are given in Mayo (1980).

(a) Using the correct T–τ relation, for various relevant values of (T, g), given by Gingerich (1969) in place of equation (9) and our procedure gave fluxes very close to the Gingerich values. The error for $\lambda > 3000$ Å was negligibly small, and was $\lesssim$ factor 2 by 1500 Å. This implies that in the optical our basic procedure works and the accuracy is limited by the use of the approximate T–τ relation (9). The error in the UV is mainly due to non-inclusion of scattering in the source function and certain high temperature opacities.

(b) For the line profiles our procedure produced negligible differences at $T = 10^4$ K, $\log g = 4$ and $T = 25\,000$ K, $\log g = 6$ when compared with Gingerich (1969) and Wickramasinghe (1972) profiles.

4.7 DOPPLER BROADENING

To account for Doppler broadening due to the rotation of the disc each annulus was divided up into 20 azimuthal (ϕ) sectors, though because of symmetry only 10 points were evaluated (*cf.* Fig. 2). In any sector the velocity V_{obs} as seen by the observer is given by the projection of the local Keplerian circular velocity, V_K, about the central object of mass M_*

$$V_{obs} = V_K \sin\phi \sin i = \left(\frac{GM_*}{R}\right)^{1/2} \sin\phi \sin i, \tag{14}$$

and ϕ satisfies $-\pi/2 \leqslant \phi \leqslant \pi/2$.

For the continuum the velocity effect, though small, was included. Its main effect is to broaden absorption edges at wavelength λ by $\pm\Delta\lambda$ (Å) where.

$$\Delta\lambda \sim \frac{\lambda V_K \sin i}{c} \sim 10\,\text{Å}. \tag{15}$$

For the lines the Doppler broadening is an important broadening mechanism and it was included in detail. The line profiles were computed by (i) summing up Doppler shifted zero velocity profiles from each sector and (ii) adding up the emergent intensity at those different rest wavelengths in each sector on the disc which gave the same observed wavelengths. There was no difference in results of the two approaches.

5 Calculation of *UBV* colours

The flux, F_ν from equation (13), received at Earth from the continuum only, was transformed into *UBV* colours since these are the main observational data available for cataclysmic variables and suchlike objects.

5.1 TRANSFORMATION

The fluxes were folded into the UBV response functions in the manner described by Matthews & Sandage (1963) for 1 and 2 airmass and were then corrected to absolute *UBV* colours above the atmosphere. Some small changes in the transformation equations were made to improve agreement with standard star colours (Willstrop 1965). The equations used, in the usual notation, were

$$(U-B) = 0.921\,(u-b)_1 - 1.308, \tag{16}$$

$$(B-V) = (b-v)_0 + 0.925. \tag{17}$$

For some discs the approximate absolute visual magnitude, M_V, was computed by using the received flux near 5500 Å. The zero point was such that $M_V = 0$ corresponded to a flux of 3.72×10^{-9} erg s^{-1} cm^{-2} Å^{-1} at 5451 Å.

5.2 PROBLEMS WITH COLOURS WHEN COMPARING OBSERVATIONS AND THEORY

There are several problems involving colours when comparing observations and theory and we discuss 'worst cases'. (i) The *U* colour is sensitive to metal line-blanketing which we neglected. (ii) The *U* band is sensitive to exact details of the flux near the Balmer jump at 3647 Å. Including higher order Balmer absorption lines can decrease the *U* flux (i.e. increase the *U* colour) by up to 0.2 mag. (iii) The *B* band especially is affected by the lower order Balmer lines in absorption or emission. Tests using fluxes from Gingerich (1969) show that for a $T = 10^4$ K, $\log g = 4$ (A0 star) atmosphere the inclusion of lower order hydrogen absorption lines changes the colours by $\delta(B-V) = +0.10$ and $\delta(U-B) = -0.06$. We note, however, that for dwarf novae in outburst the hydrogen absorption lines are not as strong as in an A0 star and they often contain emission components which reduce the effect on colours of the absorption lines. In this case the errors due to neglect of (ii) or (iii) are small. This does not hold for dwarf novae in quiescence. (iv) Convection was neglected in our atmosphere models. But tests using Gingerich (1969) fluxes showed that any error in colours is $\leqslant 0.01$ mag. (v) In one disc model (Section 6.3.2) the disc was continued using blackbodies at temperatures cooler than 5000 K. Real model atmospheres at those temperatures contain strong absorption lines and bands which significantly change our computed colours by amounts of order $\Delta(B-V) \sim 0.1$ mag and $\Delta(U-B) \sim 0.7$ mag.

Table 3. Parameters for model discs.

Model	M_* ($M_\odot$)	R_1 (10^9 cm)	F (10^{16} g s^{-1})	R_2 (10^{10} cm)	T_{e_2} ★ (K)	Comments
a1	1.0	1.0	60	1	18 500	
a2				2.48	10 000	
b1	1.0	1.0	0.6	0.44	10 000	
b2				0.48	9 514	
b3				0.52	9 048	
b4				0.62	8 088	
b5				0.76	7 083	
b6				0.86	6 527	
b7				0.96	6 065	
b8				1	5 901	
c1	0.5	1.5	0.6	0.25	10 000	$T \sim 10^4$ K is nearly the maximum temperature, $T < 10^4$ K for $R < 1.8 \times 10^9$ cm
c2				1	4 800	
d1	0.65	1.0	3.8	0.76	10 100	To compare with SCR
d2				2.05	5 140	
d3				3.73	3 400	

★ See footnote to Table 2.

6 Continuum results

The procedure described in Sections 3, 4 and 5 was used to compute the spectrum of several different accretion discs. Table 3 gives the model disc parameters. The disc is specified by M_*, R_1, F and R_2, though R_1 is, in principle, fixed by M_*. R_2 was varied. Each disc was computed with several values of the inclination angle, i, $i = 0$, 30, 60, 80, 85 and 89° (edge on).

6.1 FLUX DISTRIBUTION

The overall flux distribution for disc b1 is given in Fig. 3 for the different values of i and for $R_2 = R_2(T = 10^4\,\mathrm{K})$. These results are typical for all the discs and illustrate the general

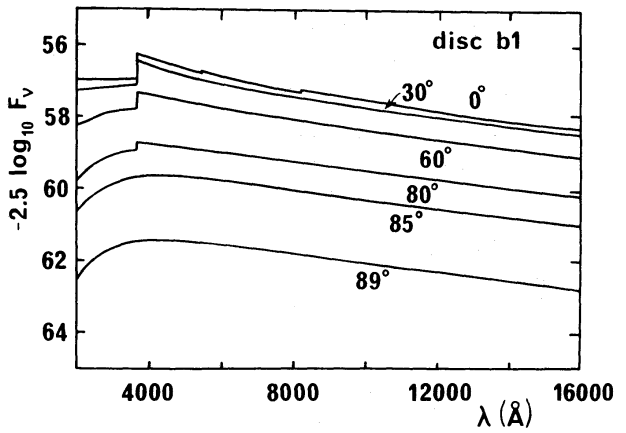

Figure 3. The continuum spectrum of disc b1 at various inclination angles.

features. At $\lambda < 3000$ Å the results are very approximate (*cf.* Section 4.2). The main features of Fig. 3 are:

(i) The approximate power law continuum $F_\nu \propto \nu^\beta$ with $\beta \sim 0.35$ for $\lambda \gtrsim 4000$ Å (this is seen better in Fig. 7). The slope is very close to the value $\beta = 0.33$ found by using the blackbody distribution (Section 2) and confirms the accuracy of the whole numerical procedure.

(ii) The variation in continuum flux as a function of i, not only because of the $\cos i$ projection factor in equation (13) but also because of atmospheric limb darkening. The total limb darkening is particularly severe at $\lambda \lesssim 3000$ Å. Table 4 (see below) separates out the projection and atmospheric limb darkening effects.

(iii) The Balmer jump is noticeably affected by the limb darkening. Defining a Balmer jump index $J = -2.5 \log [F_\nu(\lambda = 3638\text{ Å})/F_\nu(\lambda = 3658\text{ Å})]$ then, as i goes from 0° through to 89°, J takes the values 0.70, 0.62, 0.42, 0.16, 0.06 and 0.03 mag respectively.

(iv) Other disc models give results broadly similar to Fig. 3. The details depend on what is kept fixed and what is varied and can be understood (and predicted) by noting the (T, g) properties of the atmospheres making up the disc. This is best illustrated by reference to effects on *UBV* colours (see Section 6.2.2).

Further details for disc b1 of limb darkening are given in Table 4 and shown in Fig. 4. The total disc limb darkening is obtained from the ratio $F_\nu(\mu)/F_\nu(\mu = 1)$ from equation (13) and refers directly to the values plotted in Fig. 3. The effect of the atmosphere alone is obtained by removing the projection factor $\cos i$. Note that the integrated fluxes across the disc have been used and so the limb darkening is an average value for the whole disc. The results refer only to the continuum, lines are not included. The main results from Table 4 are that the $\cos i$ projection factor is more important than the atmosphere alone and that the Eddington approximation is not very accurate.

The other disc models give results broadly similar to those in Table 4. Increasing R_2 adds cooler material and increases the severity of the limb darkening (i.e. decreases $F_\nu(\mu)/F_\nu(\mu = 1)$). Increasing F and increasing M_* both decrease the severity of the limb darkening (i.e. increase $F_\nu(\mu)/F_\nu(\mu = 1)$).

Fig. 4 shows the limb darkening as a function of μ, with and without the $\cos i$ projection effect, for discs b1 and b8 and for the Eddington approximation.

6.2 *UBV* COLOUR RESULTS

6.2.1 M_V

Table 5 gives the values of M_V for several discs. As a function of i the numbers give further values of limb darkening effects (*cf.* Table 4). The table shows that the absolute visual

Table 4. Values of total disc and atmospheric only limb darkening for disc b1.

Limb darkening quantity★	Wavelength (Å)	Inclination angle 0°	30°	60°	80°	85°	89°
Total	5451	1	0.81	0.43	0.14	0.066	0.013
Atmospheric only	5451	1	0.93	0.86	0.78	0.76	0.74
Total	4340	1	0.81	0.40	0.12	0.055	0.011
Atmospheric only	4340	1	0.93	0.81	0.67	0.63	0.60
Eddington approximation	—	1	0.92	0.70	0.50	0.45	0.41

★ Total is given by $F_\nu(\mu)/F_\nu(\mu = 1)$ with $F_\nu(\mu)$ from equation (13)
Atmosphere only is given by $(F_\nu(\mu)/\mu)/F_\nu(\mu = 1)$
The Eddington approximation is $I_\nu(\mu)/I_\nu(\mu = 1) = 0.6(\mu + 2/3)$.

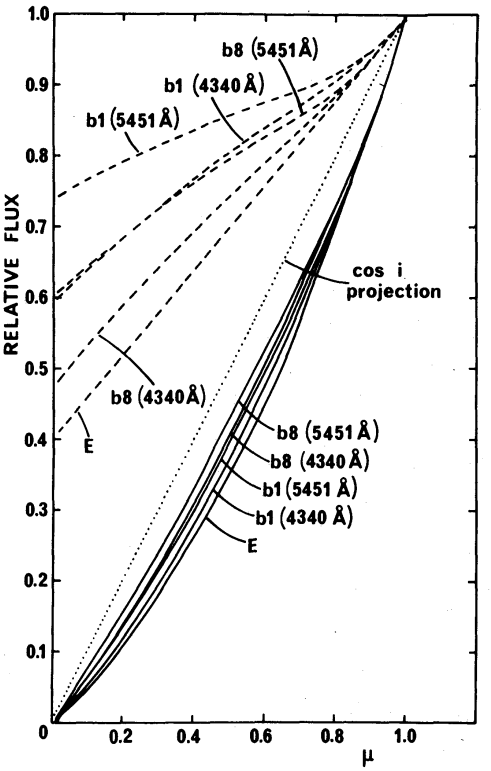

Figure 4. Limb darkening for discs b1 and b8 at wavelengths 5451 Å and 4340 Å. The full lines give the total disc limb darkening effect, i.e. the relative flux $F_\nu(\mu)/F_\nu(\mu = 1)$. The dashed lines remove the cos i projection factor and give the atmosphere components only i.e. $(F_\nu(\mu)/\mu)/F_\nu(\mu = 1)$. The Eddington approximation is labelled E and is shown with and without the cos i projection factor which is shown as a dotted line.

Table 5. M_V for several discs.

Disc i (°)	c1	c2	b1	b8	a1	a2
0	10.3	8.4	8.2	7.4	4.9	4.0
30	10.5	8.7	8.4	7.7	5.1	4.2
60	11.3	9.5	9.1	8.4	5.7	4.9
80	12.6	10.9	10.3	9.7	6.9	6.1
85	13.4	11.7	11.1	10.6	7.7	6.9
89	15.2	13.5	12.9	12.3	9.5	8.7

magnitudes of discs can extend over a wide range of values. Comparing values for discs c1 and c2, b1 and b8 and a1 and a2 shows that increasing R_2 increases the visual flux as expected. The amount is of order a factor 2 to 6 for the parameters chosen here. The values for disc c1 show that the visual flux from a disc can be small and of order that of a white dwarf ($M_V \sim 10$–15 mag). The visual flux increases dramatically as F increases, however, comparing discs b8 and a1, which have the same value of R_2 but different values of F, shows that increasing F by a factor 100 produces an increase in V flux by a smaller factor of order 10. This is because disc a1 is everywhere hotter than disc b8 and much of its flux is radiated at shorter wavelengths, i.e. a bolometric correction effect.

The results shown in Table 5 are in general agreement with the calculations of Bath *et al.* (1974) and Herter *et al.* (1979).

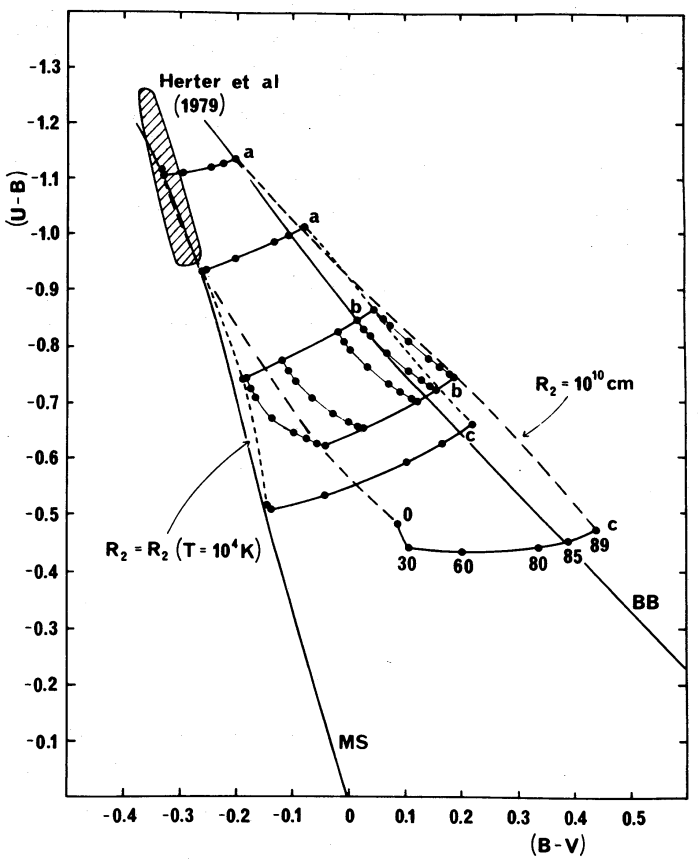

Figure 5. Theoretical $(U-B)$–$(B-V)$ diagram for the discs a, b and c described in Table 3. The outer boundaries at $R_2 = 10^{10}$ cm and $R_2 = R_2$ ($T = 10^4$ K) are indicated. For disc b the intermediate values are also shown. The inclination angle i increases from left to right for all discs as shown at the bottom for disc c. The main-sequence and blackbody lines are shown. The shaded box encloses the region discussed by the Rochester group (Herter *et al.* 1979).

6.2.2 Colours

Fig. 5 is a $(U-B)$–$(B-V)$ two-colour diagram which summarizes the theoretical results for discs a, b and c of Table 3. We first note that values for $i = 0°$ may be somewhat inaccurate because of the effect of the Balmer jump on the U-band. The main features of the diagram are:

(i) the general disc region lies roughly between the main-sequence (Allen 1973) and blackbody (Arp 1961) lines. This is expected since the optical light is dominated by an average of atmospheres whose fluxes are in between main-sequence and blackbody values. Also as i increases, limb darkening causes a reddening in $(B-V)$ and as $i \to 90°$ the Balmer discontinuity disappears and the colours approach the blackbody line.

(ii) The colours are sensitive to the size of the disc (R_2). Increasing R_2 adds cooler material which reddens the colours. The effect is quite large and is more or less independent of F and M_*. Several values of R_2 are shown for disc b. For discs a and c only $R_2 = 10^{10}$ cm and R_2 where $T = 10^4$ K are given. Note that for disc a, $R_2(T_e = 10^4\,\mathrm{K}) > R_2 = 10^{10}$ cm whereas the converse is true for discs b and c. This is because disc a is much hotter everywhere due to the large mass flux rate, F. For discs b and c, in going out from $R_2(T_e = 10^4$ K) to $R_2 = 10^{10}$ cm, $(B-V)$ and $(U-B)$ both increase by about 0.15 mag, on continuing to $R_2 \sim 3.8 \times 10^{10}$ cm (not shown in diagram) the effect is smaller since the added material is so

much cooler that it contains little radiation in *UBV* bands. The large colour change between $R_2(T_e = 10^4\ \mathrm{K})$ and $R_2 = 10^{10}$ cm shows why it is important to decide where the disc edge is.

(iii) Increasing F alone causes T_e to increase everywhere ($T_e \propto F^{1/4}$, equation 1). This causes a bluer disc.

(iv) Decreasing M_* alone causes T_e to decrease everywhere ($T_e \propto M^{1/4}$, equation 1). This causes a redder disc. There is a gravity effect too but it mainly affects the line profiles.

(v) Increasing i alone cause $(B-V)$ to redden and $(U-B)$ to become bluer. This is because the B flux decreases faster than the V flux and the Balmer jump diminishes altering the U band value. Essentially as i increases the limb darkening makes the spectrum more blackbody-like.

(vi) Also plotted in Fig. 5 are the overall results of Herter *et al.* (1979) including their disc 2 for which $F = 63 \times 10^{16}\ \mathrm{g\,s^{-1}}$ $(10^{-8} M_\odot\ \mathrm{yr^{-1}})$, $M_* = 1 M_\odot$ $R_1 = 5 \times 10^8$ cm, $R_2 = 1.82 \times 10^{10}$ and $i = 0$–$60°$. This model is comparable in detail to our disc a and considering the vast difference in stellar atmospheres used the agreement is good.

6.3 COMPARISON WITH OTHER THEORETICAL WORK

6.3.1 Herter et al. (1979)

This group (their Fig. 14 and their Table 8) using procedures outlined in Table 1 have calculated disc colours which populate the box shown in Fig. 5. We suggest the difference between these results and ours is because their discs are in general very much hotter than ours. For example their model disc 6 has $M = 1 M_\odot$, $R_1 = 5 \times 10^8$ cm, $F = 10^{-7} M_\odot\ \mathrm{yr^{-1}} = 631 \times 10^{16}\ \mathrm{g\,s^{-1}}$ and $R_2 = 8.9 \times 10^9$ cm. These data give (equation 1) for their disc edge T_e $(R_2 = 8.9 \times 10^9\ \mathrm{cm}) \sim 40\,000$ K. Now main-sequence stars with $T \sim 40\,000$ K (and $\log g = 4$) have $(B-V) \simeq -0.35$ and $(U-B) \simeq -1.15$ and small Balmer jump (Allen 1973). Proceeding towards the disc centre, as T increases, $(B-V) \rightarrow -0.4$ and $(U-B) \rightarrow -1.3$. Thus the resultant overall disc colour $((U-B) = -1.26$ $(B-V) = -0.37$ $(i = 0°))$ is consistent and expected.

We have discussed in Section 6.2 (vi) the reasonable agreement in the overlap region with Herter *et al.* disc model 2, which is almost their reddest one, with our discs a1 and a2. We also note that our disc a2 with $R = R_2(T = 10^4\ \mathrm{K})$ has Balmer jump values very similar to those of Herter *et al.* disc 2.

The fact that the model discs of Table 3 cover a broader and cooler region of the two colour diagram (Fig. 5) compared with the models of Herter *et al.* (1979) is mainly because of our considering smaller values of M_* and F and larger values of R_2.

6.3.2 Schwarzenberg-Czerny & Rózyczka (SCR)

Schwarzenberg-Czerny & Rózyczka (1977) using procedures outlined in Table 1 have computed disc colours for rather large discs. We have attempted to reproduce their results by using disc model d in Table 3. Inclination angles $\cos i = 0.25$, 0.5 and 0.9 were used. We used three values of R_2, namely (i) $R_2 = 7.6 \times 10^9$ cm corresponding to $T_e = 10^4$ K, (ii) $R_2 = 2.05 \times 10^{10}$ cm and (iii) $R_2 \sim 3.8 \times 10^{10}$ cm, the value used by SCR. The first two cases are computed using the usual procedure and provide further information on the effects of R_2 on disc colours. However, in model (iii) the temperature falls below 5000 K and our atmosphere procedure fails. We used blackbodies for $T < 5000$ K and the disc edge is at $T \sim 3400$ K.

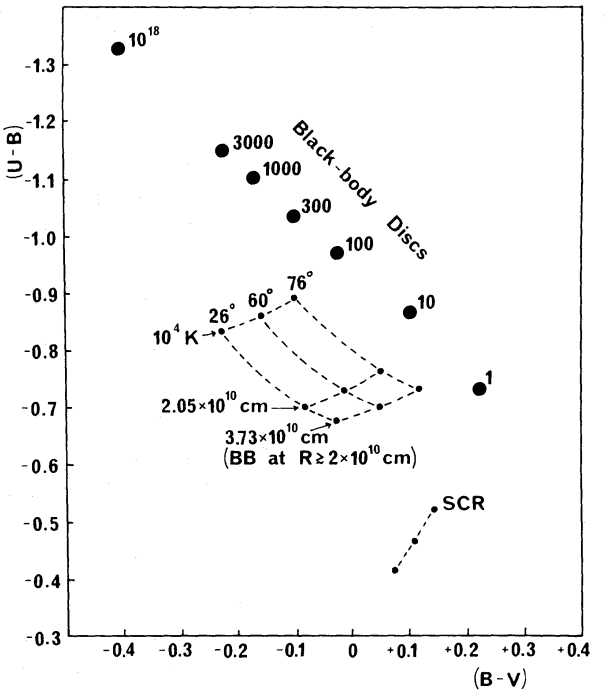

Figure 6. Theoretical $(U-B)$–$(B-V)$ diagram for comparison with the results of Schwarzenberg-Czerny & Rózyzcka (SCR). The discs are labelled with R_2 or T_{e_2} and the values of i are shown. The large circles give the values of blackbody discs labelled by the mass transfer rate in units of $10^{-10}\,M_\odot\,\mathrm{yr}^{-1}$.

The colours of the SCR discs are shown in Fig. 6 and are quite different from ours. The difference is 0.2 mag in $(U-B)$ and 0.05 mag in $(B-V)$. We suspect that the discrepancy is caused by the different procedures used for the atmospheres at $T < 5000$ K. Since the disc goes out to $T \sim 3400$ K a significant fraction of the disc is in this cool state. Our use of blackbodies neglects the effects of lines and bands which (Section 5.2 (v)) gives us much more U flux.

We again note that since results are quite sensitive to the treatment of the cool outer part of the disc it is vital to decide the value of R_2.

At high mass flux rates, $F \gg 200\times10^{16}\,\mathrm{g\,s^{-1}}$, the colours computed by SCR approach those of us and Herter *et al.* (1979) in the top left-hand corner of the two-colour diagram. We suggest that this is because even with as large a disc as $R_2 \sim 4\times10^{10}$ cm, as SCR have, for $F \gg 200\times10^{16}\,\mathrm{g\,s^{-1}}$, the temperature is everywhere $\gg 10^4$ K and the colour values converge.

We performed one further comparison with the results of SCR. We computed disc d (with variable F) with the emergent radiation in each annulus given by a blackbody instead of a stellar atmosphere. We took $R_2 = 3.8\times10^{10}$ cm and $F = (1, 10, 100, 300, 1000, 3000$ and $10^{18})\times10^{-10}\,M_\odot\,\mathrm{yr}^{-1}$. The agreement with SCR is perfect in the sense that our points lie on the 'blackbody disc' line in their Fig. 2. This suggests that the overall disc and colour programs are in good agreement. The value $F = 10^8\,M_\odot\,\mathrm{yr}^{-1}$ is simply an artifact to construct a very hot ($T \sim 10^8$ K) disc. These blackbody discs have colours which also agree, within differences due to R_2, with the blackbody calculations of Steiner (1979).

7 Comparison of theory and observation for continuum and colours

7.1 APPLICABILITY OF THE MODEL

The main restriction assumed in our calculations is the constancy of the mass flux rate. Given a constant mass flux input at the disc outer edge, constancy throughout the disc can

be considered to be set up on the time-scale of order that for matter to flow radially through the disc, which is (Shakura & Sunyaev 1973, equations 2.16 and 2.19)

$$t \sim (0.1-1)\alpha^{-4/5} \text{ day} \quad (18)$$

for $M = 1 M_\odot$, $F_{16} \sim 100$ and $R_2 \sim 10^{10}$ cm. Thus for $\alpha \sim 1$ a constant mass flux throughout the disc (in response to constant input) is a good approximation for events lasting of order a day or more. However, for small values of α the time to set up mass–flux constancy can be very long (of order years).

The problem of a time dependent rate of mass–flux through a disc has been considered by Pringle (1974), Lynden-Bell & Pringle (1974) and discussed with regard to dwarf novae outbursts by Bath *et al.* (1974). One result is that on a fairly short time-scale a disc structure very roughly that of the steady-state approximation is set up. The evolution, roughly speaking, is a 'wave' of material moving inwards through the disc which is spreading out. This can be modelled approximately by adjusting R_2 and considering only those annuli which contain the bulk of the mass.

The UX UMa disc stars (Warner 1976b) and dwarf novae at standstill seem stable for time-scales of years and thus may be considered steady-state. The application of the model to dwarf novae at outburst ($\Delta t \sim 2$ day) is probably reasonable, based on observational justification. The time-scale for the outburst is only a few days which implies that the accretion also occurs on that time-scale so the viscosity parameter itself must be high.* Thus subject to the caveat of quasi-steady state, dwarf novae in outburst can be considered by the current model.

For dwarf novae in quiescence ($\Delta t \sim 30$ day) a steady-state disc can in principle be set up in the time between outbursts (*cf.* observations of the emission lines in Z Cha which extend down to near the surface of the white dwarf, Rayne (1980), thus implying that a disc exists). However, in quiescence the light from the disc may be swamped by that from the hot spot, red star and white dwarf (*cf.* Tylenda 1977). Thus only shorter period systems for which the other components contribute very little may in certain cases be described by the disc models.

7.2 CONTINUUM

Over the wavelength range ($\lambda \gtrsim 3000$ Å) that our disc models are reliable the continuum slope (*cf.* Fig. 3) is rather insensitive to i, F, M_* and R_2. Thus only a very general comparison is possible. Fig. 7 shows spectrophotometry of the dwarf nova EX Hya in quiescence obtained by G. T. Bath and Mayo at AAT on 1979 January 9. 62 (UT). The infrared 2.2 μm value is from M. Sherrington (private communication). The solid curves are disc b8 ($R_2 = 10^{10}$ cm, $i = 60°$) and disc a2 ($R_2 = (T = 10^4$ K), $i = 60°$). Since EX Hya has very short period (98 min) and shows no evidence of a bright spot we expect that even at quiescence the disc dominates the light so that comparison with the results here is meaningful.

The general change in slope caused by increasing mass flux rate, F, is clear – radiation from hotter regions is added which alters the slope, especially in the ultraviolet. For $\lambda \gtrsim 4000$ Å the fit to the data by both discs b8 and a2 is good. For $\lambda < 4000$ Å the theoretical continuum of disc b8 drops below the observed value, whereas disc a2 lies above the observations. Thus a value of F somewhere in between discs a and b will fit both the UV and optical parts of the disc ($F_{16} \sim 5$, say). We have not fitted the 2.2 μm point in detail as there may be a contribution there from a free–free continuum.

* We must be consistent here. Our models with $Z_0(R)/R = 0.05$ have small α. This does not affect colours much when compared with $Z_0(R)/R = 0.01$ ($\alpha \sim 1$), but for line profiles the effect can be serious (see Section 8).

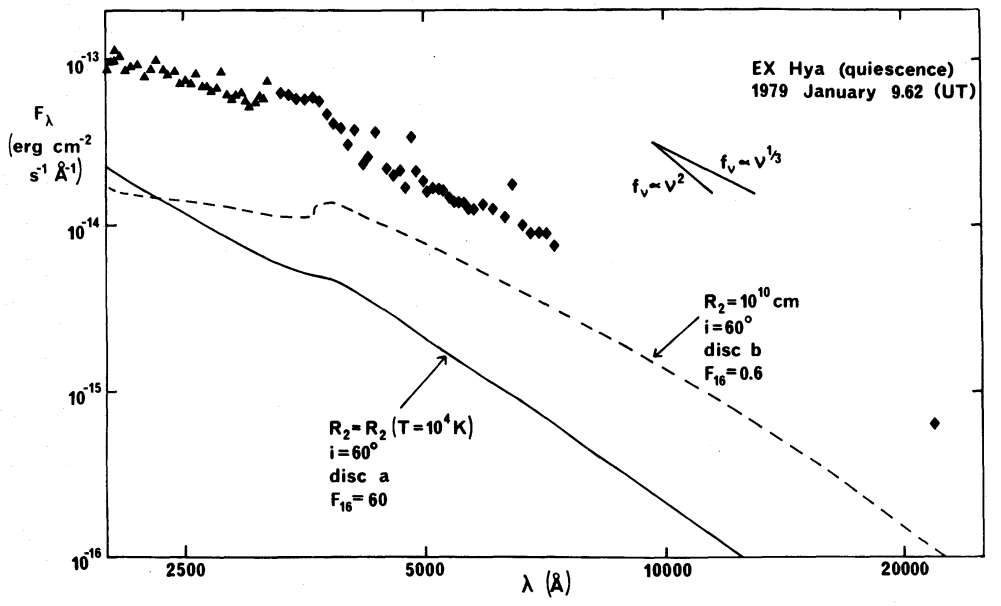

Figure 7. Comparison of continuum disc spectra with observations of EX Hya. The plot is on a logarithmic scale, and power law slopes $F_\nu \propto \nu^{1/3}$ and $F_\nu \propto \nu^2$ are shown. $F_\nu \propto \nu^\alpha$ implies $F_\lambda \propto \lambda^{-(2+\alpha)}$. The F_λ scale refers to the observed data. The theoretical lines can be shifted vertically by an arbitrary amount corresponding to changes in distance. F_{16} is the mass flux rate in units of 10^{16} g s^{-1}.

7.3 COMPARISON OF *UBV* COLOURS

7.3.1 M_V

Fig. 8 plots the values of M_V for the discs of Table 5 against i and compares these with observations of various objects. The data for novae (N), recurrent novae (RN) and dwarf novae (DN) in outburst (O) and quiescence (Q) and UX UMa stars are taken from Warner (1976a,b), Robinson (1976), Bailey (1979) and Wade (private communication). There is some uncertainty in the quoted values. The data for stars is from Allen (1973).

In view of the uncertainties in the absolute quantities in our computations (as opposed to ratios) we do not wish to overinterpret Fig. 8. However, it is clear that the values computed for M_V for the high mass flux disc, disc a, lie near the observed outburst values of M_V for dwarf novae and the observed values of M_V for the UX UMa stars. The values of M_V for the low mass flux discs, disc b and disc c, lie near the observed quiescent dwarf nova values. The observed change in M_V from quiescence to outburst in a dwarf nova is of order 3–5 mag in rough agreement with discs b and a in Fig. 8.

7.3.2 Colours

Fig. 9 is the observational two-colour diagram which includes the outline of the region spanned by our theoretical disc models of Figure 5. The main-sequence (MS) and blackbody (BB) lines are as in Fig. 5.

All (except one) points plotted are observed (i.e. reddened values.) Most of the objects are nearby ($\lesssim 300$ pc) and we expect the interstellar reddening $E(B-V) < 0.10$ mag. The dereddening correction vector of length $E(B-V) = 0.1$ mag is shown. One plotted point (A) for Nova Mon–A0620 – 00 at outburst has been dereddened by $E(B-V) = 0.4$ mag.

The data shown are for UXUMa disc stars, dwarf novae in outburst and the evolution of some dwarf novae from quiescence to outburst. They have been collected from several sources: Warner (1976a, Tables IV and V), Warner (1976b), French (1975, for A0620), Hill

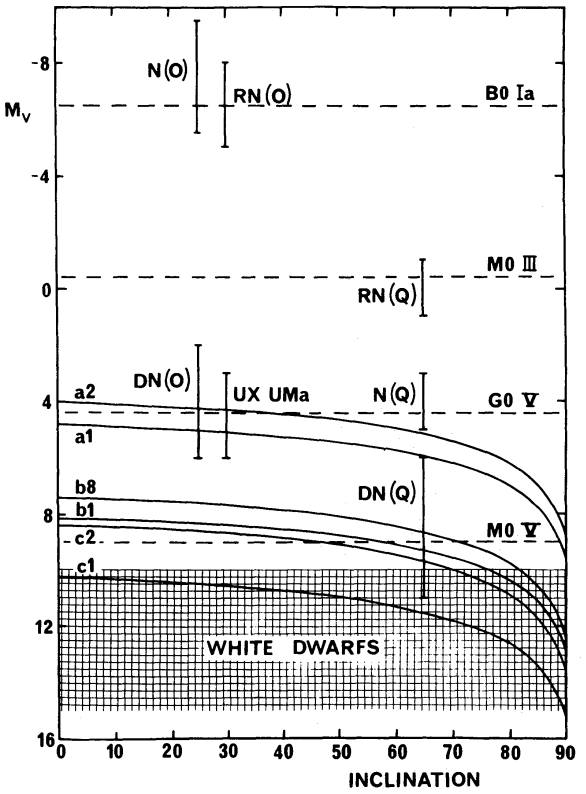

Figure 8. Theoretical absolute magnitudes M_V of discs as a function of inclination angle. The observed ranges of values of novae (N), recurrent novae (RN) and dwarf novae (DN) in quiescence (Q) and outburst (O) and UX UMa 'disc' stars are plotted. Several typical single stars are plotted for comparison purposes. The observed system data is plotted near the middle of the diagram since it is at unknown inclination angle (though we suspect that the range of observed values is partly due to inclination effects).

(1970, for CD–42°14462), Vogt (1974), Marino & Walker (1978) and the compilations by Haefner, Schoembs & Vogt (1979), Bailey (1979) Walker & Marino (1978) and Zuckermann (1961) for the treks of U Gem, SS Cyg, VW Hyi and Z Cam through the two-colour plane, based on original data referenced in those papers.

The label (Q) refers to quiescence, (O) to outburst peak and (SO) to superoutburst peak. For the observations of Z Cam and U Gem the outburst peak could not be determined and it lies somewhere near the top of the trajectory. In comparing observations and theory it is important to use colours near the peak of the outburst since the steady-state approximation is best then and the disc is 'full'. (Of course to use the bolometric rather than optical peak is more correct, but unavailable at present.) For this reason we did not plot colours for all dwarf novae outbursts given in the literature since many of these in fact refer to the decline stage when the disc is rather empty with the matter wave near the centre, thus being hot and not as luminous.

In order not to further crowd the diagram no old novae are plotted nor other dwarf novae at quiescence. In general these lie near the quiescent values shown already.

The main features of Fig. 9 in comparing theory and observations are:

(i) the rather small amount of available *UBV* colour data for dwarf novae through outburst; we urge more work on this difficult observational problem.

(ii) The dwarf novae in outburst generally lie in the region of the two-colour diagram populated by the theoretical models of Section 6. We interpret this as evidence, both that the disc indeed dominates the light in such systems and that the theoretical models of

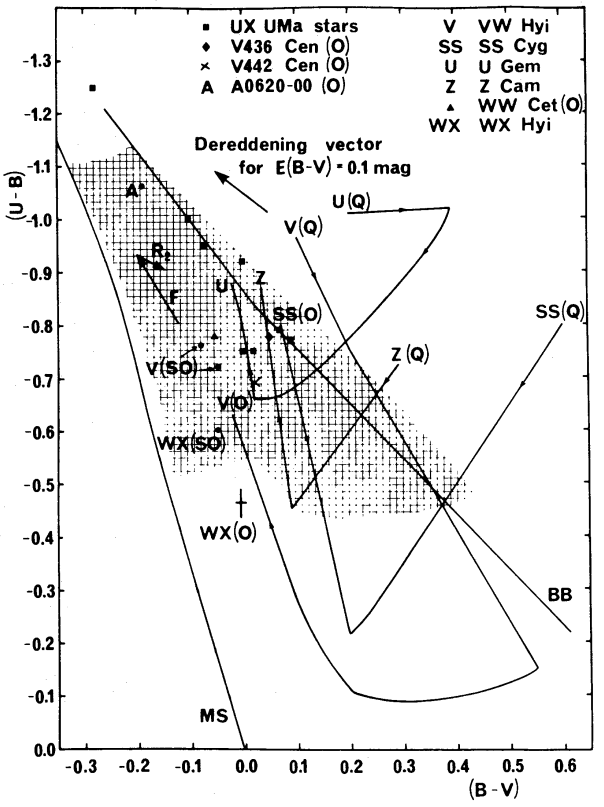

Figure 9. Observational $(U-B)-(B-V)$ diagram. MS is the main-sequence and BB the blackbody line. The theoretical disc area (from Fig. 5) is shown as a shaded area. Q, O, SO refer to quiescent, outburst and superoutburst. The tracks show U Gem, Z Cam, SS Cyg and VW Hyi from quiescence to outburst. Vectors F and R_2 refer to increases by a factor 4 in F and 1.5 in R_2. The de-reddening vector is given for $E(B-V) = 0.1$ mag.

Section 6 are generally confirmed by the observations. Note that the blackbody discs (Section 6.3.2) are not in agreement with observations.

(iii) The UX UMa stars are a subset of the cataclysmic variables which show broad shallow absorption lines and are thought to contain a disc (Warner 1976a, b). They also lie in or near the disc region of Fig. 9. We regard this as further evidence that the disc is indeed the dominant light source in such systems. It is not clear if the UX UMa's are old novae that went unrecorded or are dwarf novae 'permanently' stuck in an outburst state (e.g. like a Z Cam standstill).

(iv) Dwarf novae in quiescence, and old novae, in general do not lie in the disc region of the two-colour diagram. This is expected since the colours of such systems are usually dominated by the red star, bright spot and/or white dwarf.

Some further comments can be made which require more detailed interpretation of Fig. 9.

(v) In comparing the outburst and superoutburst of the same dwarf nova, it is clear that M_*, R_1, and i must be fixed. There is probably some difference in values for R_2 with the superoutburst value being larger owing to its having a longer time ($\Delta t \sim 10$ day) to spread the disc. This leaves the mass flux rate F as the main parameter to be changed. For both VW Hyi and WX Hyi the V magnitude at superoutburst is larger than at outburst by about 0.6 mag. This can be produced by an increase in F by a factor of about 4. (There is uncertainty here because of the details of the bolometric correction which depends on the actual temperatures in the disc.) The vector labelled F in Fig. 9 shows roughly how the

Table 6. Change in colours from outburst to superoutburst

Object	ΔV	$\Delta(B-V)$	$\Delta(U-B)$
VW Hyi	−0.55	−0.05	−0.11
WX Hyi	−0.65	−0.04	−0.13
Model disc F increased by factor 4	−0.6	−0.08	−0.13

colours of a disc change when F is increased by a factor 4. The theoretical expected changes in colours are collected in Table 6 along with the observed ones for VW Hyi and WX Hyi. The observed values are averages of two values. The agreement with theory is good for $\Delta(U-B)$ but not for $\Delta(B-V)$. This is because the observed vector in the two-colour diagram is more nearly vertical than that due solely to an increase in F. We note that the discrepancy in $\Delta(B-V)$ can be removed by allowing R_2 to increase somewhat in the superoutburst case. The vector in the two-colour diagram caused by changing only R_2 is shown next to that labelled F and a combination of these two vectors can produce the observed more nearly vertical movement in the two-colour diagram along a line of constant inclination. Thus the observed colour differences between the outburst and superoutburst of a dwarf novae are in detailed agreement with the disc model.

We suggest therefore that in the superoutburst state the rate of mass flux through the disc is about four times larger than in the outburst state and that the optically thick part of the disc is larger, possibly by about 50 per cent.

(vi) The trek through the two-colour diagram of a dwarf nova on its rise to outburst can also be interpreted in terms of the disc models (*cf.* Bath *et al.* 1974; Pringle 1974). Shortly after the rise has begun the colours became redder; this may be interpreted as the outer cooler parts of the disc dominating the light. As the mass transfer wave moves in through the disc, the main radiating part of the disc becomes hotter and hence bluer. Viscosity also spreads out the disc and R_2 increases. The matter wave moves further in causing a continuing bluer colour. In particular, during the latter part of the rise and near the peak, the disc may be in a quasi steady state and the movement should be roughly similar to that joining outburst to superoutburst (i.e. movement roughly along a line of constant i but with effects due to R_2 increasing).

Finally, much of the matter wave has accreted, the disc empties and declines in luminosity and the colours return to a state of being dominated by other parts of the system. In this general way the tracks in Fig. 9 may be explained (*cf.* Bailey 1979).

(vii) As a final comment on Fig. 9 we note that Herter *et al.* and SCR have found that their calculated colours disagree with the observed ones. Both sets of authors also state that the theory and observation can probably be reconciled by considering additional continuum radiation due to the secondary, the boundary layer, reprocessed radiation and the optically thin chromosphere.

However, the discussion in Section 6.3 shows that the situation is much simpler than this. We suggest that the discs computed by Herter *et al.* (1979) will agree with observations if they are extended further out to cooler parts and if lower mass flux rates and central masses are used. In fact Herter *et al.* noted that the early termination of their discs was a major deficiency in their calculation. Similarly we suggest that SCR discs cut off at $T \gg 3000$ K will show better agreement with observations.

Finally, we note that the additional sources of continuum radiation suggested by Herter *et al.* (1979) and SCR are actually small when compared with the disc at outburst (*cf.* Tylenda (1977) for the boundary layer and bright spot; Pacharintanakul & Katz (1979) for reprocessing; Warner (1976a) for red star compared with disc; and in outburst the line

(absorption or emission) contribution to colours is small). However, the effects mentioned are all important when the dwarf nova is quiescent. Reprocessing may be important for *line* emission at outburst also.

8 Calculated and observed line profiles of discs

8.1 THEORETICAL RESULTS

Using the method described in Sections 4.5 and 4.7 we have computed the Hα, Hβ and Hγ absorption profiles for discs a, b and c of Table 3. The results are shown in Fig. 10(a)–(c), for the case where $R_2 = R_2$ ($T_e = 10^4$ K). The parameter values full width at half maximum (FWHM) and central depth (d_c) are plotted in Figs 12 and 11. Hγ is asymmetric because

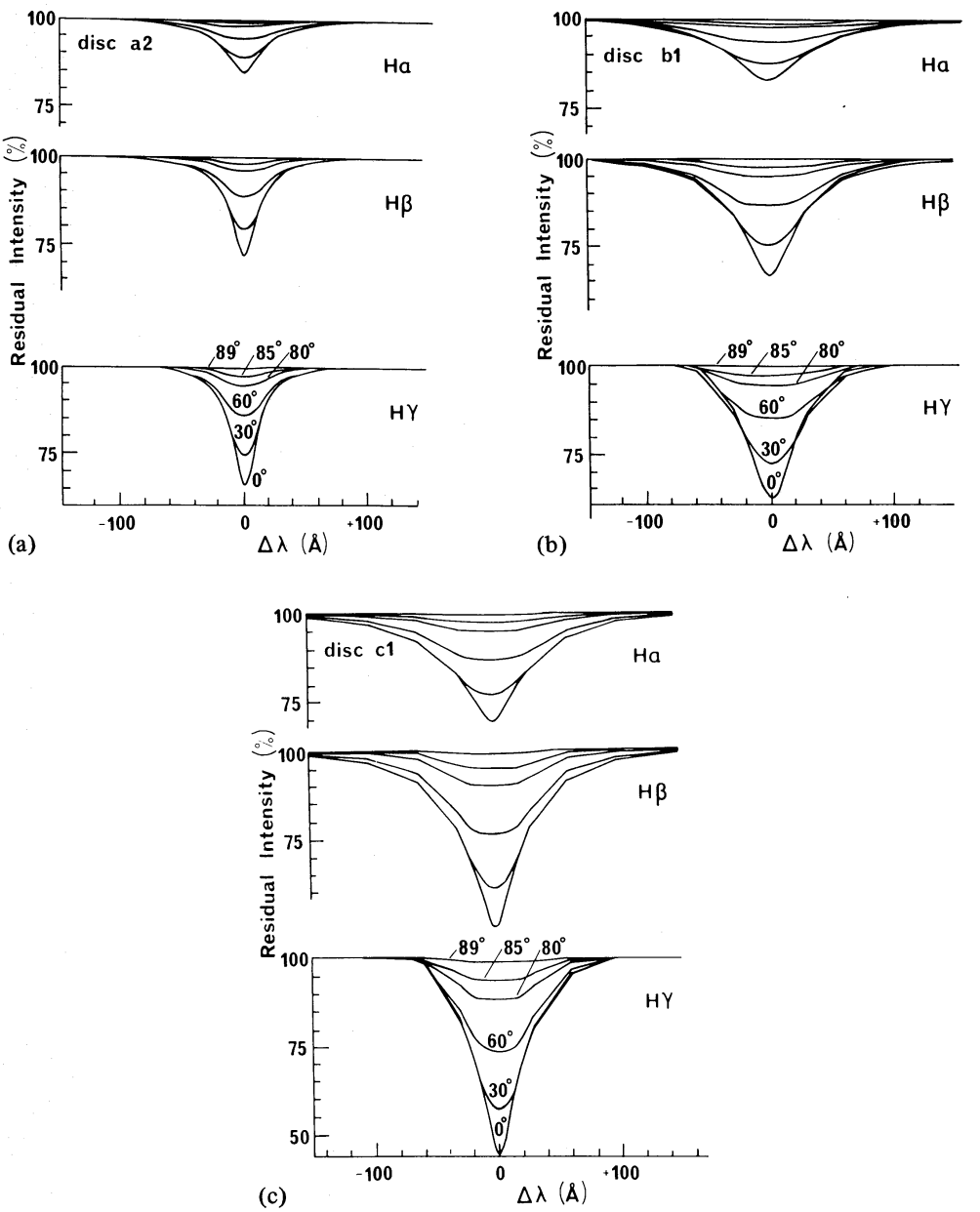

Figure 10. (a) Hydrogen line profiles for disc a2 ($R_2 = R_2$ ($T = 10^4$ K)). (b) As (a) but for disc b1. (c) As for (a) but for disc c1.

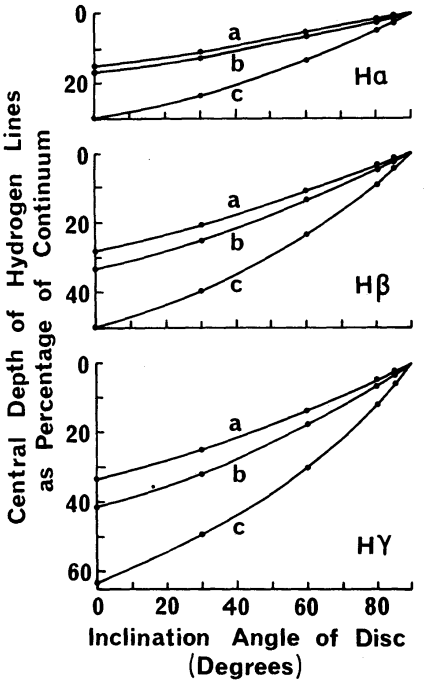

Figure 11. Central depth of hydrogen lines as a function of inclination angle for discs a2, b1 and c1.

its blue wing is affected by the wing of Hδ. We have approximately allowed for this and drawn a symmetric Hγ profile, and the values of d_c in Fig. 11 are measured from the asymmetric profile. The main results are:

(i) For all values of M_*, i and F considered here $d_c(H\gamma) > d_c(H\beta) > d_c(H\alpha)$.

(ii) The lines are very broad and shallow. (FWHM ~ 100 Å, FWZI ~ 150 Å, d_c ~ 20 per cent). The two contributors are Stark (pressure) broadening because of the high surface gravities in the disc ($\log(g_Z) \sim 5$–6) and rotational broadening because of the Keplerian

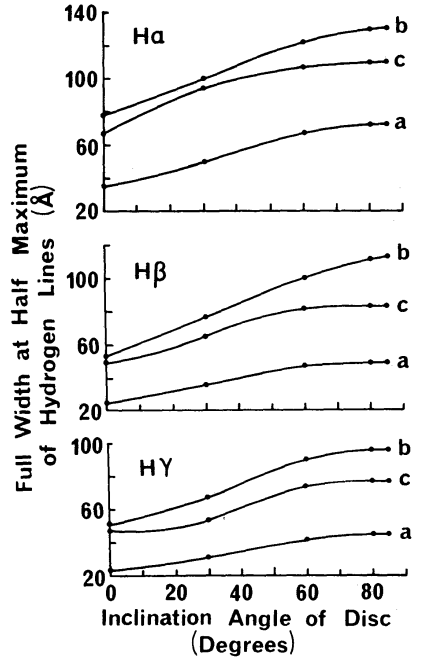

Figure 12. FWHM of hydrogen lines as a function of inclination angle for discs a2, b1 and c1.

rotation of the disc $V_K \sim 1000\,\mathrm{km\,s^{-1}}$). The relative contribution of these effects depends on the exact conditions in the disc and in particular at what radius the dominant line forming region occurs. An estimate can be obtained from Fig. 13(a) which compares line profiles for Hβ with and without Doppler broadening.

(iii) At fixed i and M_*, increasing F decreases both d_c and FWHM. This follows because $T_e \propto F^{1/4}$, so at any given disc radius the temperature is higher. This tends to decrease the line strength (provided $T \gtrsim 10^4$ K). In discs with fixed cut-off radius at R_2 ($T_e = 10^4$ K), the effect is diluted since material out to R_2 ($T = 10^4$ K) is included in both discs. (One could imagine an opposite effect in comparing a very cool disc ($T \ll 10^4$ K everywhere) with a hotter one ($T \sim 10^4$ K) with larger F value). The radius at which the Balmer lines are strongest (R_2 ($T \sim 9000$ K)) increases as F increases. Thus the surface gravity in the line forming region decreases causing less pressure broadening and the Keplerian velocity decreases causing less Doppler broadening. Both effects decrease the FWHM of the line as F increases.

(iv) At fixed i and F reducing M_* increases d_c and decreases FWHM. Since $T_e \propto M_*^{1/4}$ the argument about d_c of (iii) holds. The effect on the FWHM is more complicated. The gravity at fixed radius decreases so the pressure broadening decreases and a reduced M_* decreases the rotational broadening at fixed radius. However, there is a competing effect because as M_* decreases the dominant line-emitting region moves inwards causing both increased pressure and rotational broadening.

(v) At fixed M_* and F, as i increases, the lines become weaker. This is because, as i increases, the flux in each annulus from continuum and line become more equal since each is formed at parts of the atmosphere physically closer to one another giving smaller temperature difference between the regions of continuum and line formation.

(vi) The result of (v) may be altered by the inclusion of scattering in the source function. We have neglected it and it may produce emission cores in the absorption lines (*cf.* Gorbatskii 1964; Mihalas 1970).

(vii) Fig. 13(b) shows the change in Hβ line profiles for disc b, with $R_2 = R_2$ ($T_e = 10^4$ K) when $Z_0(R)/R = 0.05$ (equation 3) is replaced by $Z_0(R)/R = 0.01$. There is a reduction in

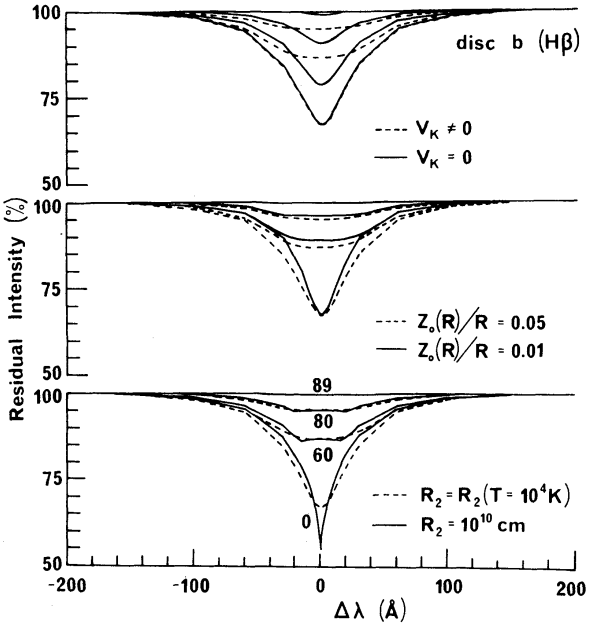

Figure 13. Theoretical Hβ line profiles for disc b under various changes: (a) Doppler broadening; (b) disc height; (c) disc outer radius. Note that in the top panel the dotted and solid lines coincide at $i = 0$.

gravity by a factor 5 which has a noticeable effect on the line profiles. The lines are much less broad in the low gravity case and also somewhat weaker.

We have tried to compare our line results with those of Herter *et al.* (1979). For our disc a and their disc model 2 (Table 5 of Herter *et al.*) and making allowance for different values of $Z_0(R)/R$ we find at least moderate agreement at $i \gtrsim 30°$. But at $i = 0°$ there may be some differences possibly because of the coarseness of our numerical scheme.

(viii) Fig. 13(c) shows the final effect we considered for disc b, the change of disc edge from R_2 ($T_e = 10^4$ K) to $R_2 = 10^{10}$ cm. The main effect is to add in extra line forming material at lower effective gravity. For small i this causes the line to strengthen and become narrower. Note in particular at $i = 0°$ the sharp core reminiscent of white dwarf line shape. At $i \gtrsim 60°$ the effect is smaller and mainly on the line width.

8.2 OBSERVATIONAL DATA

Since 1976 we have been observing dwarf novae and similar objects spectroscopically using the AAT. A brief summary has been given elsewhere (Whelan *et al.* 1979). In this time we have caught a few outbursts by chance, but with help from monitoring by amateur astronomers. The line profiles during outburst may be compared with the theoretical line profiles of Section 8.1. The journal of observations is given in Table 7. This includes an indication of what part of the outburst was caught based on the outburst visual monitorings of the Variable Star Section, Royal Astronomical Society of New Zealand (Bateson 1976, 1978, and private communication). Table 7 includes A0620 – 00 a recurrent novae whose spectrum resembles that of a dwarf nova and a UX UMa 'disc' star CD–42° 14462 (Warner 1976b) which has also been observed by Wegner (1972). In Table 7 the 1978 October data for VW Hyi were obtained by H. C. Arp, C. C. Brunt and J. A. J. Whelan using the Schectman detector on the Las Campanas 100-in. Du Pont telescope and the spectrum of A0620 was obtained with the AAT and Robinson–Wampler (1972) scanner by D. A. Allen (*cf.* Whelan *et al.* 1977). The remainder of the data have been obtained by subsets of the present authors using the AAT with the IPCS (Boksenberg 1972) (1977, 1978 data) and with the Robinson–Wampler scanner (1976 data).

8.3 COMPARISON OF OBSERVATIONS AND THEORY

There are several parameters in the disc models (M_*, F, i, R_2) so that it is often possible to select a theoretical line profile which agrees reasonably with observations. However, to be consistent in comparing theory and observation, it is necessary to consider disc models which also produce the correct colours and satisfy any other constraints available.

Table 7. Journal of line profile observations

Object	Date (UT)	Equipment and resolution	Comments
CD–42° 14462	1977 May 16	AAT, IPCS, 1.5 Å	UX UMa 'disc star'.
VW Hyi	1976 Aug 24	AAT, IDS, 9 Å	Outburst, near peak.
	1978 Oct 23	Du Pont 100 in., Schectman system, ~10 Å	12 day superoutburst, near peak
	1978 Nov 21	AAT, IPCS, 6.5 Å	Outburst, on decline.
Z Cha	1978 Nov 21	AAT, IPCS, 6.5 Å	Superoutburst, on rise.
	1978 Nov 22	AAT, IPCS, 1.5 Å	Superoutburst, at peak.
V436 Cen	1976 Apr 29	AAT, IDS, 9 Å	12 day superoutburst, 3 days after peak.
A0620 – 00	1976 Jan 14	AAT, IDS, 4.5 Å	Recurrent nova, on decline 164 days after outburst.

The following discussion is meant to illustrate the general principles involved. We note that in general the observed line profiles are somewhat asymmetric so we have averaged them, and that the profile in the extreme wing ($\Delta\lambda \gtrsim 40$ Å) is strongly influenced by errors in setting the continuum.

8.3.1 CD–42° 14462

CD–42° 14462 is a UX UMa disc star (Warner 1976b; Wegner 1972). The observations suggest that the brightness of this object has not changed much on a time-scale of order $\gtrsim 10$ yr. Thus any disc in this system is likely to be in a steady-state and to have spread out to an equilibrium size. We assume that $Z_0(R)/R \sim 0.05$ is all right and that R_2 may be large. The absence of eclipses demands $i \lesssim 80°$.

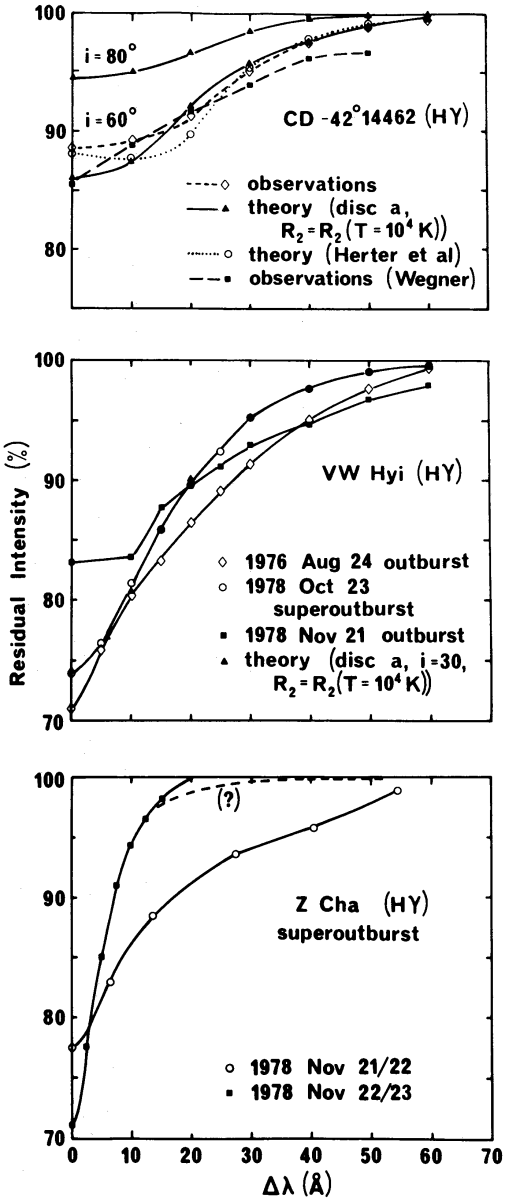

Figure 14. Theoretical and observed Hγ line profiles for (a) CD–42° 14462; (b) VW Hyi; (c) Z Cha. In the middle panel the symbols ○ and ▲ often overlap producing a symbol ●. This is due to the close agreement of observation and theory.

In the $(U-B)$–$(B-V)$ diagram the colours of CD–42° 14462 are consistent with $80° > i \gtrsim 60°$, and disc b, $R_2 = 10^{10}$ cm or more and $F \gg 0.6$ or disc a, $R_2 \sim R_2$ ($T = 10^4$ K), $F < 60$. This suggests that the sort of disc to consider has $M_* \sim 1 M_\odot$, large F and large R_2.

Measurements of the Hγ line from the observations reported in Table 7 are summarized in Fig. 14(a) together with several theoretical profiles. The observed lined profile is characterized by $d_c \sim 12$ per cent and FWHM ~ 50 Å. The theoretical line profiles for disc a, $i = 60°$, 80°, $R_2 = R_2$ ($T = 10^4$) are also shown in Fig. 14(a). The $i = 60°$ case fits the observations well in the wings, but is somewhat deeper at $\Delta\lambda \sim 0$. We suggest that the agreement is reasonable and note (i) there may be emission in the core of the observed line; and (ii) increasing i by a small amount brings the theoretical core of the line into agreement, with observations and then simultaneously decreasing F by a small amount keeps the wings fixed.

Also plotted in Fig. 14(a) are the line profile ($i = 60°$) from Herter *et al.* disc model 1 (their Fig. 15) and the observed Hγ profile from Wegner (1972). The Herter *et al.* disc profile agrees well with our observations in the wings but deviates in the core. The Wegner (1972) observed profile differs substantially from our observed profile suggesting variability. We could not fit the Wegner data.

8.3.2 VW Hyi

Again we consider the Hγ line profile. The outburst colours suggest the following possibilities: (i) disc b, $i \sim 50°$, $R_2 \sim 10^{10}$ cm; (ii) disc a, R_2 very large so that the disc edge has $T \ll 10^4$ K; (iii) disc c with F large, and $i \sim 60$. Fig. 14(b) shows three observed profiles of VW Hyi. We consider first the general shape of the superoutburst and 1976 August outburst profiles. The wings are noticeably concave downwards which, comparing Fig. 10(a) and (b), argues for a high mass flux disc; we reject possibility (i).

To consider possibility (ii) we find that the line profile for disc a, $i = 60°$ $R_2 = R_2$ ($T = 10^4$ K) fits the data reasonably well. But such a disc has colours very different from those of VW Hyi at outburst. Increasing R_2 to improve colour agreement weakens the agreement of the line profiles in the wings.

We are thus led to consider possibility (iii), a high mass flux, lower central mass disc. We have not computed line profiles for such a disc but we found (*cf.* Fig. 10b, c) that disc c at $i = 60°$ has a very similar line profile to disc b at $i = 30°$. To estimate the line profile of disc c at $i = 60°$ with a high mass flux rate we assume it is roughly the $i = 30°$ profile of disc b at a high mass flux rate, namely disc a, which is plotted in Fig. 14(b). There is almost perfect agreement between this approximate theoretical profile and the superoutburst observations.

In the above we assumed $Z_0(R)/R = 0.05$ but for dwarf novae in outburst a lower value may be more appropriate (*cf.* Section 7.1) and this affects the line profiles (*cf.* Fig. 13c). The above discussion is not intended to be conclusive but to illustrate the procedure, and the fact that using *both* colour and line profile information can constrain the theoretical parameters permitted by the observations.

The difference between the superoutburst and 1976 August outburst profile can be straightforwardly explained by comparing Fig. 10(a) and (b). The main difference (for $\Delta\lambda \gtrsim 10$ Å) can be accounted for by increasing F by a factor of order 3 to 10 (and possibly also R_2) from the outburst to superoutburst profile. This is in detailed agreement with the colour effects discussed in Section 7.3 (v).

The 1978 November outburst profile of VW Hyi is very different from the other two. As yet we cannot explain it. However, we note that: (i) in that spectrum there was no Hα

absorption; (ii) the outburst had passed its peak; and (iii) next night there was moderately strong emission in Hγ. We suspect that there is weak emission in the core ($\Delta\lambda \lesssim 20$ Å) of the profile shown in Fig. 14(b) and that the disc radiation output may be dominated by the higher gravity inner parts, thus strengthening the wings (*cf.* Fig. 13c).

8.3.3 Z Cha

The Z Cha dwarf nova system has been extensively studied (Warner 1974; Bath *et al.* 1974; Bailey 1979; Fabian *et al.* 1979, Rayne 1980). These papers provide constraints such as $i \sim 73°$, $M_* \sim 0.5 M_\odot$. No outburst colours are available. The observed profiles of Hγ during the 1978 November superoutburst are plotted in Fig. 14(c). That on November 22/23 is remarkable for its narrowness and may have an extensive very weak wing; the Hδ profile does. The spectrum also shows absorption lines of He I (λ 4471) and Ca II *K* (λ 3933) with somewhat shallower profiles. The presence of Ca II implies the existence of a cool region suggesting the disc is optically thick in its outer very cool parts.

We have not yet been able to fit this narrow observed profile theoretically, but we indicate, briefly, the sort of disc which might work. To obtain such a narrow profile we need rather low gravity in the line forming region. This suggests that $Z_0(R)/R$ is small (*cf.* Section 7.1 and Fig. 13b), $M_* \lesssim 0.5 M_\odot$, and R_2 is very big (*cf.* Fig. 13c). The latter is reasonable, since at high F value (during superoutburst) R_2 must be large to reach as low as T as ~ 6000 K to see the Ca II *K* line. Since the data were obtained near the start of the superoutburst it is possible that the light is then dominated by material near the disc edge. Note that this argument cannot be pushed too far because of the He I λ 4471 line which requires $T \gtrsim 15\,000$ K. Further theoretical disc calculations are required to test these ideas and could be additionally compared with the spectra of SS Cyg through outburst described by Hinderer (1949) and Zuckermann (1961).

8.3.4 V436 Cen and A0620 – 00

Fig. 15 shows the observed outburst Hβ line profiles of V436 Cen and A0620 – 00. In both cases the broad absorption line is dominated by strong emission. For both objects very roughly the flux in the emission line in outburst is of the same order as at quiescence. This suggests that the emission is not due only to a scattering core. Subtracting out the emission line gives an Hβ absorption profile with $d_c \sim 8$ per cent and FWHM ~ 50 Å suggesting a hot, high gravity, moderate inclination disc. We present these data to show that in outburst the recurrent X-ray nova A0620 – 00 is like the dwarf nova V436 Cen in outburst and that the

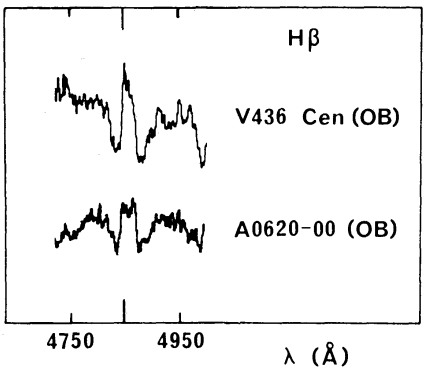

Figure 15. Observed Hβ line profiles for A0620 – 00 and V436 Cen.

problem of emission in the absorption lines cannot be solved by the present investigation and must be remembered when interpreting the results of Fig. 14(a)–(c).

9 Conclusion

The calculations reported here contain several uncertainties caused by ignorance or approximation. The main unknowns are the disc $Z_0(R)$ structure and its outer boundary, R_2. The agreement of the continuum results with theoretical blackbody disc spectra and with Herter *et al.* (1979) (colours and Balmer jump for their disc 2) suggests that our atmospheric approximation is valid.

In general the disc models reported here produced *UBV* colours and line profiles in moderate agreement with the observations of dwarf novae at or near outburst and UX UMa stars. This suggests that the disc indeed dominates the light output of these objects and the disc model of dwarf novae receives further support. The comparison of superoutburst and outburst colours and profiles suggests that the mass–flux rate is higher by a factor of order 4 in the former case and that there is no need to invoke such ideas as nuclear burning. This can be further tested by ultraviolet observations at $\lambda \lesssim 1500$ Å. The differences between the disc models reported here and those of Herter *et al.* (1979) and Schwarzenberg-Czerny & Rózyczka (1977) can be mainly traced to the parameters F, R_2 and $Z_0(R)/R$. The ultimate test of the theory is the observations which indicate that the broad range of parameters chosen here are reasonable. However, improved theory and data are needed before one can say, for example, that $Z_0(R)/R$ must be 0.01 rather than 0.05 with a corresponding determination of the viscosity parameter, α.

In the hope of improving the model, but remaining within its simple framework, we are currently investigating two further aspects: (i) the He I (λ 4471) and Ca II *K* (λ 3933) line profiles are being computed to give separate constraints on the hotter and cooler parts of the disc. In this way the disc structure may be sampled at three(including hydrogen) places with different characteristic temperatures. Further, the Ca II *K* profile will give information on the outer part of the disc and hence R_2; and (ii) moving a matter wave through a disc to simulate a quasi-steady approximation to a time-dependent disc in the hope of explaining in detail the trek of a dwarf-nova through the two-colour plane.

Further *UBV* and spectroscopic observations and consideration of the UV both theoretically and observationally are also important.

The main result of this paper is that the colours and line profiles of dwarf novae in outburst can be satisfactorily modelled by a steady-state accretion disc.

Acknowledgments

SKM is grateful for an SRC Research Studentship held during part of this work. We acknowledge the support of the Computer Centres at Cambridge and RGO. We are grateful for access to data provided by F. M. Bateson and H. Arp. We acknowledge useful discussions with J. E. Pringle, D. Lynden-Bell, S. M. Rucinski, B. E. J. Pagel, A. Kiplinger, E. L. Robinson, J. Bailey, F. Wesemael, R. E. Williams, R. A. Wade and G. T. Bath.

References

Allen, C. W., 1973. *Astrophysical Quantities,* 3rd edn, Athlone Press, London.
Aller, L. H., 1963. *Atmospheres of the Sun and Stars,* p. 332, Ronald Press, New York.
Arp, H., 1961. *Astrophys. J.,* **133**, 874.
Bailey, J., 1979. *Mon. Not. R. astr. Soc.,* **187**, 645.

Bateson, F. M., 1976. *Mon. Circ., Var. Star Sect. R. astr. Soc. N.Z., M76/4, M76/5, M76/8.*
Bateson, F. M., 1978. *Mon. Circ., Var. Star Sect. R. astr. Soc. N.Z., M78/10, M78/11, M78/12.*
Bath, G. T., Evans, W. D., Papaloizou, J. & Pringle, J. E., 1974. *Mon. Not. R. astr. Soc.*, **169**, 447.
Boksenberg, A., 1972. *Proc. ESO & CERN Conference on Auxiliary Instrumentation for Large Telescopes,* Geneva, p. 295.
Cayrel, R. & Traving, G., 1960. *Z. Astrophys.*, **50**, 248.
Elvey, C. T. & Babcock, H. W., 1943. *Astrophys. J.*, **130**, 99.
Fabian, A. C., Pringle, J. E., Whelan, J. A. J. & Bailey, J. A., 1979. *IAU Coll. 46, New Trends in Variable Star Research,* p. 65, eds Bateson, F. M. *et al.*, Hamilton, New Zealand.
French, H., 1975. *IAU Circ. 2835.*
Gingerich, O. W., 1969. *Theory and Observations of Normal Stellar Atmospheres,* M.I.T. Press.
Gorbatskii, V. C., 1964. *Astr. Zh.*, **41**, 849; English translation, *Soviet Astr. A. J.*, **8**, 680 (1965).
Griem, H. R., 1964. *Plasma Spectroscopy,* McGraw-Hill, New York.
Haefner, R., Schoembs, R. & Vogt, N., 1978. *ESO Preprint No. 33.*
Herter, T., Lacasse, M. G., Wesemael, F. & Winget, D. E., 1979. *Astrophys. J. Suppl.*, **39**, 513.
Hill, P. W., 1970. *Trans. IAU XIVB,* 235.
Hinderer, F., 1949. *Astr. Nachr.*, **277**, 193.
Lynden-Bell, D., 1969. *Nature,* **223**, 690.
Lynden-Bell, D. & Pringle, J. E., 1974. *Mon. Not. R. astr. Soc.*, **168**, 603.
Kiplinger, A. L., 1977. *Bull. Am. astr. Soc.*, **9**, 633.
Kiplinger, A. L., 1979. *Astrophys. J.*, **234**, 997.
Marino, B. F. & Walker, W. S. G., 1978. *Publs Var. Star Sect. R. astr. Soc. N.Z.*, **6**, 66.
Matthews, T. A. & Sandage, A. R., 1963. *Astrophys. J.*, **138**, 49.
Mayo, S. K., Wickramasinghe, D. T. & Whelan, J. A. J., 1979. *IAU Coll. 46, New Trends in Variable Star Research,* p. 52, eds Bateson, F M. *et al.* Hamilton, New Zealand.
Mayo, S. K., 1980. *PhD Thesis,* in preparation, University of Cambridge.
Mihalas, D., 1970. *Stellar Atmospheres,* p. 330. Freeman, San Francisco.
Novikov, I. D. & Thorne, K. S., 1973. *Black Holes,* p. 204, ed. De Witt, C. & B. S., Springer-Verlag, New York.
Osterbrock, D. E., 1974. *Astrophysics of Gaseous Nebulae,* Freeman, San Francisco.
Pacharintanakul, P. & Katz, J. T., 1980. *Astrophys. J.*, **238**, 985.
Pringle, J. E. & Rees, M. J., 1972. *Astr. Astrophys.*, **21**, 1.
Pringle, J. E., 1974. *PhD Thesis,* University of Cambridge.
Pringle, J. E., 1977. *Mon. Not. R. astr. Soc.*, **178**, 195.
Rayne, M. W., 1980. *PhD Thesis,* University of Cambridge.
Robinson, E. L., 1976. *A. Rev. Astr. Astrophys.*, **14**, 119.
Robinson, E. L., Nather, R. E. & Patterson, J., 1978. *Astrophys. J.*, **219**, 168.
Robinson, L. B. & Wampler, E. J., 1972. *Publs astr. Soc. Pacif,* **84**, 161.
Schwarzenberg-Czerny, A. & Rozyczka, M., 1977. *Acta astr.*, **27**, 429.
Smak, J., 1971. *Acta astr.*, **21**, 15, and *IAU Coll. 15, New Directions and New Frontiers in Variable Star Research,* p. 248, Veröff Rerneis Sternwarte Bamberg IX.
Shakura, N. I. & Sunyaev, R. A., 1973. *Astr. Astrophys.*, **24**, 337.
Steiner, J. E., 1979. Preprint.
Tylenda, R., 1977. *Acta astr.*, **27**, 235.
Vidal, C. R., Cooper, J. & Smith, E. W., 1973. *Astrophys. J. Suppl.*, **25**, 37.
Vogt, N., 1974. *Astr. Astrophys.*, **36**, 369.
Walker, W. S. G. & Marino, B. F., 1978. *Publs Var. Star Sect. R. astr. Soc. N.Z.*, **6**, 73.
Warner, B., 1976a. *IAU Symp. 73, Structure and Evolution of Close Binary Stars,* p. 85, eds Eggleton, P. *et al.*, Reidel, Dordrecht.
Warner, B., 1976b. *Observatory,* **96**, 49.
Wegner, G., 1972. *Astrophys. Lett.*, **12**, 219.
Whelan, J. A. J., Ward, M. J., Allen, D. A., Danziger, I. J., Fosbury, R. A. E., Murdin, P. G., Penston, M. V., Peterson, B. P., Wampler, E. J. & Webster, B. L., 1977. *Mon. Not. R. astr. Soc.*, **180**, 657.
Whelan, J. A. J., Rayne, M. W. & Brunt, C. C., 1979. *IAU Coll. 46, New Trends in Variable Star Research,* p. 39, eds Bateson, F. M. *et al.*, Hamilton, New Zealand.
Wickramasinghe, D. T., 1971. *PhD Thesis,* University of Cambridge.
Wickramasinghe, D. T., 1972. *Mem. R. astr. Soc.*, **76**, 129.
Williams, R. E., 1980. *Astrophys. J.*, **235**, 939.
Willstrop, R. V., 1965. *Mem. R. astr. Soc.*, **69**, 83.
Zuckermann, M.-C., 1961. *Ann. Astrophys.*, **24**, 431.

Note added in proof

B. Warner has recently informed us of an unpublished University of Cape Town (1976) MSc thesis by M. C. Koen. This thesis calculates in detail a model for the vertical structure of a disc and also the corresponding emergent continuum and Hβ absorption line profile for several discs. Where comparisons can be made, the results of Koen are in rough agreement with the ones reported here; in particular the trends in line profile shapes with changes in i, R_2 and F are similar.